

Constraints on Millicharged Neutrinos via Atomic Ionizations with Germanium Detectors at sub-keV Sensitivities

Jiunn-Wei Chen,^{1,2} Hsin-Chang Chi,³ Hau-Bin Li,⁴ C.-P. Liu,³
Lakhwinder Singh,^{4,5,*} Henry T. Wong,^{4,†} Chih-Liang Wu,^{1,4,‡} and Chih-Pan Wu¹

¹*Department of Physics, National Taiwan University, Taipei 10617, Taiwan*

²*National Center for Theoretical Sciences and Leung Center for Cosmology and Particle Astrophysics, National Taiwan University, Taipei 10617, Taiwan*

³*Department of Physics, National Dong Hwa University, Shoufeng, Hualien 97401, Taiwan*

⁴*Institute of Physics, Academia Sinica, Taipei 11529, Taiwan*

⁵*Department of Physics, Banaras Hindu University, Varanasi 221005, India*

(Dated: April 30, 2022)

With the advent of detectors with sub-keV sensitivities, atomic ionization has been identified as a promising avenue to probe possible neutrino electromagnetic properties. The interaction cross-sections induced by millicharged neutrinos are evaluated with the *ab-initio* multi-configuration relativistic random-phase approximation. There is significant enhancement at atomic binding energies compared to that when the electrons are taken as free particles. Positive signals would distinctly manifest as peaks at specific energies with known intensity ratios. Selected reactor neutrino data with germanium detectors at analysis threshold as low as 300 eV are studied. No such signatures are observed, and a combined limit on the neutrino charge fraction of $|\delta_Q| < 1.0 \times 10^{-12}$ at 90% confidence level is derived.

PACS numbers: 14.60.Lm, 13.15.+g, 13.40.Gp

The physical origin and experimental consequences of finite neutrino masses and mixings [1] are not fully understood. Investigations on anomalous neutrino properties and interactions [2] are crucial to address these fundamental questions and may provide hints or constraints to new physics beyond the Standard Model (SM). An avenue is on the studies of possible neutrino electromagnetic interactions [2–4] which, in addition, offer the potentials to differentiate between Majorana and Dirac neutrinos. The neutrino electromagnetic form factors in C, P and T-conserving theories can be formulated as:

$$\Gamma_{\text{em}}^\mu \equiv F_1 \cdot \gamma^\mu + F_2 \cdot \sigma^{\mu\nu} \cdot q_\nu, \quad \text{with} \quad (1)$$

$$F_1 = \delta_Q \cdot e_0 + \frac{1}{6} \cdot q^2 \cdot \langle r_\nu^2 \rangle, \quad \text{and} \quad (2)$$

$$F_2 = (-i) \cdot \frac{\mu_\nu}{2 \cdot m_e}, \quad \text{where} \quad (3)$$

γ^μ and $\sigma^{\mu\nu}$ are the standard QED matrices, e_0 and m_e are the electron charge and mass, respectively, $q = (q_0, \vec{q})$ is the four-momentum transfer, while the neutrino properties are parametrized by the neutrino fractional charge relative to the electron (δ_Q – commonly referred to as “neutrino millicharge” in the literature), the neutrino charge radius ($\langle r_\nu^2 \rangle$), and the anomalous neutrino magnetic moment (μ_ν) [3, 4] in units of the Bohr magneton μ_B . The F_1 and F_2 terms characterize neutrino interactions without and with a change of the helicity states, respectively. The studies of δ_Q and $\langle r_\nu^2 \rangle$ should in general be coupled to those due to SM-electroweak interactions to account for the possible interference effects among them. For completeness, we note that two additional form factors are possible [4]: the electric dipole moments in theories violating both P- and T-symmetries, and the ampule

moments in P-violating theories.

The theme of this article is to report a new direct laboratory limit on $|\delta_Q|$. The searches are based on $\bar{\nu}_e$ emitted from the nuclear power reactor via atomic ionization [5], an interaction channel considered for the first time in this process. The cross-section is derived using the Multi-Configuration Relativistic Random-Phase Approximation (MCRPPA) theory [6, 7]. As will be demonstrated in Figure 1b, the bounds on event rates from δ_Q -induced atomic interactions [$\bar{\nu}_e$ -A(δ_Q)]:

$$\bar{\nu}_e + A \rightarrow \bar{\nu}_e + A^+ + e^- \quad (4)$$

to be probed in this work (~ 1 count $\text{kg}^{-1} \text{keV}^{-1} \text{day}^{-1}$ at an energy transfer of $T \sim 0.1 - 10$ keV) far exceed those due to SM interactions as well as $\langle r_\nu^2 \rangle$ -induced processes at its current limits [8], such that these effects and their interference can be neglected in our analysis.

The origin of electric charge quantization and whether it is exact is one of Nature’s profound mysteries. Many theories [9], such as extra dimensions, magnetic monopoles, and grand unified theories, provide elegant solutions, but they remain speculative. Electric charges are quantized in SM due to $U(1)$ gauge invariance and anomaly cancellation [10, 11], implying $\delta_Q = 0$. However, charge quantization is no longer ensured in many extensions of SM [11, 12]. For example, in theories with right-handed neutrinos and Dirac mass terms, electric charge is no longer quantized and δ_Q can assume an arbitrary value due to a hidden $U(1)$ symmetry whose conserved charge is the difference of baryon and lepton numbers or $B - L$. Charge quantization can be restored by introducing additional conditions such as Majorana mass terms

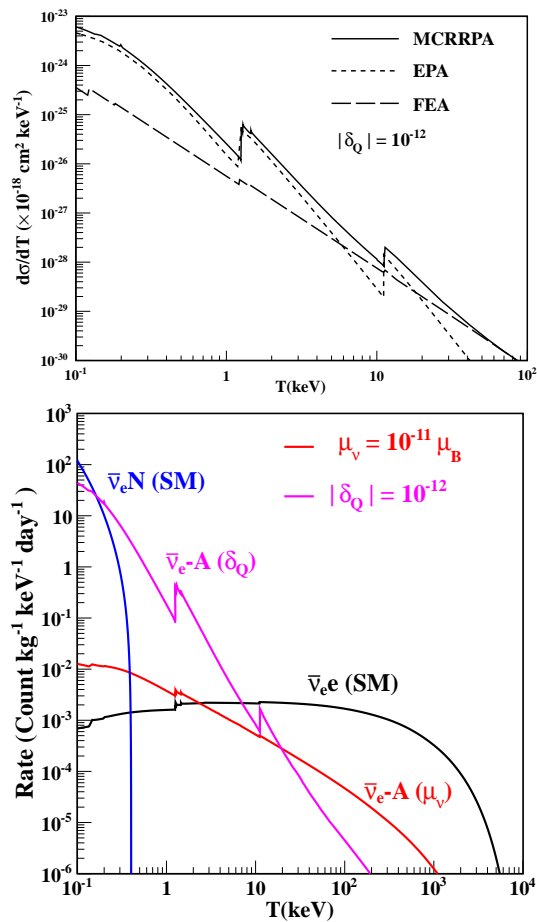


Figure 1: The differential cross-sections $\bar{\nu}_e$ -A(δ_Q) on Ge due to $|\delta_Q| = 10^{-12}$ – (a:Top) with mono-chromatic $E_\nu = 1$ MeV, derived with the FEA, EPA and MCRRA methods, and (b:Bottom) with typical reactor spectrum at a flux of $\phi(\bar{\nu}_e) = 10^{13} \text{ cm}^{-2}\text{s}^{-1}$, where contributions from SM $\bar{\nu}_e$ -e and $\bar{\nu}_e$ -nucleus(N) as well as those of $\mu_\nu = 10^{-10} \mu_B$ are overlaid. Standard quenching factors [24] are used to account for observable ionizations in nuclear recoils. The contribution to $\bar{\nu}_e$ -e from $\langle r_\nu^2 \rangle$ at its current upper bound is only a fraction of that from SM, and is not shown.

that break the $U(1)$ symmetry [11]. Neutrinos with finite charge will necessarily imply they are Dirac particles.

Model-dependent astrophysics bounds [2, 13] ranging at $|\delta_Q| < 10^{-13} - 10^{-15}$ are derived from stellar luminosity and cooling, as well as the absence of anomalous timing dispersion of the neutrino events in SN 1987A. The most stringent indirect limit is $|\delta_Q| < 3 \times 10^{-21}$ [13], inferred from constraints on the neutrality of the hydrogen atoms and the neutrons [14], and assuming charge conservation in neutron beta-decay. Earlier efforts with direct laboratory experiments placed constraints $|\delta_Q| < \text{few} \times 10^{-12}$ [15, 16] through the extrapolations of the μ_ν -results from reactor $\bar{\nu}_e$ experiments [17, 18] using simplistic scaling relationships and neglecting atomic effects.

The conventional way of evaluating the effects due to

Γ_{em}^μ is with the Free Electron Approximation (FEA). The corresponding differential cross-section for δ_Q -induced neutrino-electron scattering [15, 16] due to an incoming neutrino of energy E_ν at $T \ll E_\nu$ is:

$$\left(\frac{d\sigma}{dT}\right)_{\text{FEA}} = \delta_Q^2 \left[\frac{2\pi\alpha_{em}^2}{m_e}\right] \left[\frac{1}{T^2}\right], \quad (5)$$

where α_{em} is the fine structure constant. The $(1/T^2)$ -dependence is different from that of $(1/T)$ for μ_ν . With the advent of low-energy detectors sensitive to the energy range of atomic transitions and binding energies ($T < 10$ keV), FEA is no longer adequate and atomic ionization effects have to be taken into account [5]. Cross-sections of μ_ν -induced ν -atom scattering have been formulated [7, 19, 20] by various authors.

The cross-section $\bar{\nu}_e$ -A(δ_Q) is analogous to that induced by relativistic charged leptons, and can be described at atomic energies by the Equivalent Photon Approximation (EPA) [21]:

$$\left(\frac{d\sigma}{dT}\right)_{\text{EPA}} = \delta_Q^2 \left[\frac{2\alpha_{em}}{\pi}\right] \left[\frac{\sigma_\gamma(T)}{T}\right] \log\left[\frac{E_\nu}{m_\nu}\right], \quad (6)$$

where m_ν is the neutrino and $\sigma_\gamma(T)$ is the photo-electric cross-section by a real photon of energy T [22]. The divergence at $m_\nu \rightarrow 0$ is expected in Coulomb scattering and some cutoff schemes are necessary. The Debye length for solid-Ge ($0.68 \mu\text{m}$ or 0.29 eV), which characterizes the scale of screen Coulomb interaction, is chosen. This may introduce an uncertainty of $\sim 20\%$ to the normalization if m_ν would be replaced by other values related to neutrino mass bounds. The EPA method neglects the contributions from the longitudinal polarization of the virtual photons and hence would deviate from the correct results as T increases. It fails to describe ionizations by μ_ν , $\langle r_\nu^2 \rangle$ or electro-weak interactions [20].

We adopted the MCRRA theory [6] as an *ab-initio* approach [7] to provide an improved description of the atomic many-body effects. This becomes relevant for data from Ge detectors at sub-keV sensitivities. The MCRRA theory is a generalization of relativistic random-phase approximation by the use of a multi-configuration wave function as the reference state. The derivation is based on the time-dependent Hartree-Fock approximation. For open-shell atoms with low-lying excited state, such as Ge, double-electron excitations are automatically accounted for in MCRRA. An additional advantage is that gauge invariance of transition amplitudes is preserved. The MCRRA approach has been successfully applied to photo-excitation, photo-ionization and μ_ν -induced ionization of divalent or quasi-divalent atomic systems [6, 7]. The results are shown to match the measured photo-absorption cross-section of Ge from real photons [7]. The accuracy is within 5% at energy transfer larger than 100 eV, below which the solid state effects start to play a role, since Ge is fabricated as semiconductor crystals in ionization detectors.

| Data Set | Reactor- $\bar{\nu}_e$ Flux ($\times 10^{13} \text{ cm}^{-2} \text{ s}^{-1}$) | Data Strength Reactor ON/OFF (kg-days) | Analysis Threshold (keV) | $ \delta_Q $ 90% CL Limits ($< \times 10^{-12}$) | | |
|------------------------------|---|--|--------------------------------|--|------------------|---------------------|
| | | | | Previous Analysis | This Work FEA | This Work MCRRPA |
| TEXONO 1 kg Ge [17] | 0.64 | 570.7/127.8 | 12 | 3.7 [15] | 14 | 8.8 |
| GEMMA 1.5 kg Ge [18] | 2.7 | 755.6/187 | 2.8 | 1.5 [16] | 2.1 | 1.1 |
| TEXONO Point-Contact Ge [24] | 0.64 | 124.2/70.3 | 0.3 | — | — | 2.1 |
| Projected Point-Contact Ge | 2.7 | 800/200 | 0.1 | — | — | ~ 0.06 |

Table I: Summary of experimental limits on millicharged neutrino at 90% CL with selected reactor neutrino data. “This Work” compares data with results from FEA and MCRRPA calculations via a complete analysis, while “Previous Analysis” are based on extrapolations from μ_ν -results using simplistic scaling relations to the FEA spectra. The projected sensitivity of measurements at the specified experimental parameters is also shown.

The derived differential cross-section for $\bar{\nu}_e$ -A(δ_Q) on Ge under various schemes are depicted in Figure 1a with a mono-chromatic incident neutrino at $E_\nu = 1 \text{ MeV}$, a typical range for reactor- $\bar{\nu}_e$. The FEA scheme is expected to provide good descriptions at energy transfer larger than the atomic binding energy scale, while EPA at $q^2 \rightarrow 0$. The MCRRPA results converge to these benchmarks: $T > 50 \text{ keV}$ for FEA and $T < 1 \text{ keV}$ for EPA, confirming the method covers a wide range of validity. Two features are particularly noteworthy: (i) There is an order-of-magnitude enhancement in the MCRRPA or EPA cross-section over FEA at low energy when atomic effects are taken into account. This behaviour is opposite to that for μ_ν -induced interactions [7, 19] where the cross-section is suppressed, the origin of which is discussed in Ref. [20]. (ii) There exists a unique “smoking gun” signature for $\bar{\nu}_e$ -A(δ_Q), through the observation of K- and L-shell peaks at the specific binding energies and with known intensity ratios. Both features favor the use of detectors with low threshold at sub-keV energy, and yet possess good resolution to resolve peaks and other structures at such energy.

To be comparable with experimental data, the differential cross-sections are convoluted with the neutrino spectrum $d\phi/dE_\nu$ to provide the observable spectrum of event rates (R) as function of T :

$$\frac{dR}{dT} = \rho_e \int_{E_\nu} \left[\frac{d\sigma}{dT} \right] \left[\frac{d\phi}{dE_\nu} \right] dE_\nu, \quad (7)$$

where, ρ_e is the electron number density per unit target mass. The MCRRPA spectrum for $[\bar{\nu}_e$ -A(δ_Q)] with Ge at a typical reactor neutrino flux of $\phi(\bar{\nu}_e) = 10^{13} \text{ cm}^{-2} \text{ s}^{-1}$ is depicted in Figure 1b, and is compared with those of μ_ν -induced and SM $\bar{\nu}_e$ -e and $\bar{\nu}_e$ -nucleus coherent scatterings [23]. It can be seen that low threshold detectors can greatly enhance the sensitivities in most of the channels.

The previous analysis [15, 16] with FEA are repeated using full spectral data via standard statistical procedures. Comparisons of the results listed in Table I show discrepancies and indicate inadequacies of the scaling approach. Also displayed are the analysis of reactor $\bar{\nu}_e$ data [17, 18, 24] using the MCRRPA spectrum of Fig-

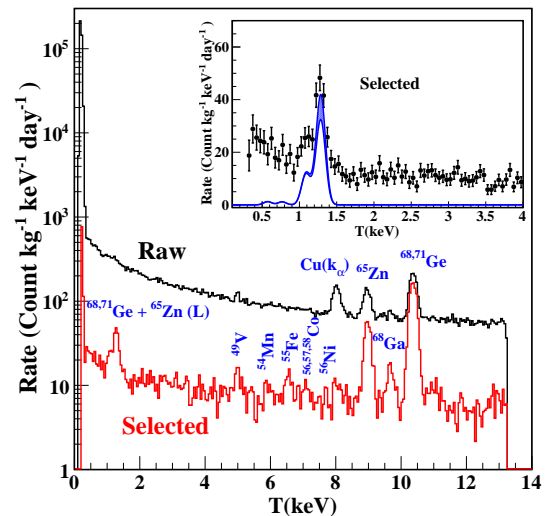


Figure 2: Typical spectra from point-contact Ge detectors at the Kuo-Sheng Reactor Neutrino Laboratory. The “Selected” spectra are due to events after having anti-coincidence with the cosmic-ray and anti-Compton detectors. The peaks are due to internal radioactivity. The low energy spectrum is expanded in the inset. Intensities of the L-shell X-rays can be independently derived from the higher-energy K-shell peaks.

ure 1b. No evidence on $\bar{\nu}_e$ -A(δ_Q) are observed and limits of $|\delta_Q|$ at 90% confidence level (CL) are derived. In particular, we illustrate the results from point-contact Ge detectors with sub-keV sensitivities at analysis threshold of 300 eV [24]. The detectors are deployed by the TEXONO experiment at Kuo-Sheng Reactor Neutrino Laboratory [8, 17] for the studies of light WIMP dark matter and $\bar{\nu}_e$ -nucleus coherent scatterings. Typical spectra are depicted in Figure 2. The “Raw” spectrum is due to all events prior to background suppression, while the “Selected” ones are those of candidate events having anti-coincidence with the cosmic-ray and anti-Compton detectors. Various lines from internal X-rays emissions due to cosmic-induced internal radioactivity can be observed. The low energy portion of the candidate spectrum is displayed in the inset. The peaks are from the L-shell X-rays, where the intensities can be quan-

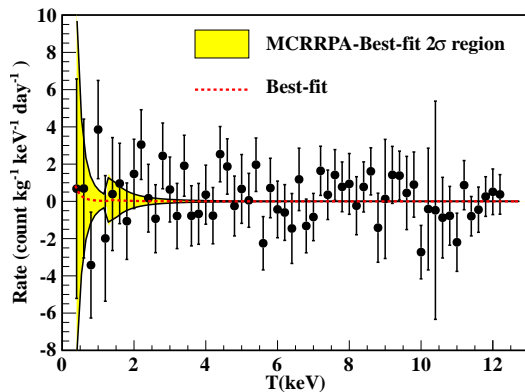


Figure 3: Analysis of $\bar{\nu}_e$ millicharge with data from point-contact Ge detectors [24], showing Reactor ON–OFF spectrum with 124.2(70.3) kg-days of ON(OFF) data. The best-fit function with its 2σ uncertainty band is superimposed.

titatively accounted for with the higher-energy K-shell peaks. Data taken in different reactor periods are combined and compared with $\bar{\nu}_e$ -A(δ_Q) from MCCRPA. Depicted in Figure 3 is reactor ON–OFF residual spectrum with 124.2(70.3) kg-days of ON(OFF) data. The best-fit solution with the 2σ uncertainty band is superimposed. A limit of $|\delta_Q| < 2.1 \times 10^{-12}$ at 90% CL is derived.

The various bounds derived from the MCCRPA analysis shown in Table I can be statistically combined. The overall limit from these reactor neutrino data is

$$|\delta_Q| < 1.0 \times 10^{-12} \quad (8)$$

at 90% CL. The projected sensitivity for a measurement at an achieved flux and data strength [18] together with 100 eV detector threshold targeted for next generation of experiments [23] would be $|\delta_Q| \sim 6 \times 10^{-14}$.

The MCCRPA theory improves descriptions on neutrino electromagnetic effects at atomic energy scales over previous techniques. Possible charge-induced interactions show enhancement at atomic binding energies, and would manifest as peaks with known intensity ratios. Novel Ge-detectors with sub-keV sensitivities and superb energy resolution are ideal to study these effects. We plan to extend our studies to neutrinos at different kinematics regimes, as well as to possible electromagnetic interactions with WIMPs as non-relativistic particles.

This work is supported by the Academia Sinica Investigator Award 2011-15 (HTW), as well as contracts 102-2112-M-001-018 (LS,HBL), 102-2112-M-002-013-MY3 (JWC,CLW,CPW), 102-2112-M-259-005 (CPL), from the Ministry of Science and Technology, Taiwan.

* Corresponding Author: lakhwinder@phys.sinica.edu.tw

† Corresponding Author: htwong@phys.sinica.edu.tw

‡ Corresponding Author: b97b02002@ntu.edu.tw

- [1] K. Nakamura and S. Petcov, Review of Particle Physics, Phys. Rev. **D 86**, 177 (2012), and references therein.
- [2] P. Vogel and A. Piepke, Review of Particle Physics, Phys. Rev. **D 86**, 622 (2012), and references therein.
- [3] B. Kayser, Phys. Rev. **D 26**, 1662 (1982); J.F. Nieves, Phys. Rev. **D 26**, 3152 (1982); R. Shrock, Nucl. Phys. **B 206**, 359 (1982); P. Vogel and J. Engel, Phys. Rev. **D 39**, 3378 (1989); H.T. Wong and H.B. Li, Mod. Phys. Lett. **A 20**, 1103 (2005); N.F. Bell et al., Phys. Rev. Lett. **95**, 151802 (2005).
- [4] C. Brogini, C. Giunti, and A. Studenikin, Adv. High Energy Phys. **2012**, 459526 (2012); C. Giunti and A. Studenikin, arXiv:1403.6344 (2014).
- [5] S.A. Fayans, V.Yu. Dobretsov and A.B. Dobrotsvetov, Phys. Lett. **B 291**, 1 (1992); G.J. Gounaris, E.A. Paschos and P.I. Porfyriadis, Phys. Lett. **B 525**, 63 (2002); H.T. Wong, H.B. Li and S.T. Lin, Phys. Rev. Lett. **105**, 061801 (2010), erratum arXiv:1001.2074v3 (2010).
- [6] K.N. Huang, W.R. Johnson, Phys. Rev. **A 25**, 634 (1982); K.N. Huang, Phys. Rev. **A 26**, 734 (1982).
- [7] J.W. Chen et al., Phys. Lett. **B 731**, 159 (2014), and references therein.
- [8] M. Deniz et al., Phys. Rev. **D 81**, 072001 (2010).
- [9] O. Klein, Nature **118**, 516 (1926).; P.A.M. Dirac, Proc. R. Soc. **A133**, 60 (1931); J.C. Pati and A. Salam, Phys. Rev. **D10**, 275 (1974); H. Georgi and S.L. Glashow, Phys. Rev. Lett **32**, 438 (1974).
- [10] R. Foot et al., Mod. Phys. Lett. **A 5**, 2721 (1990); R. Foot, H. Lew, and R.R. Volkas, J. Phys. **G 19**, 361 (1993).
- [11] K.S. Babu and R.N. Mohapatra, Phys. Rev. Lett. **63**, 938 (1989); Phys. Rev. **D 41**, 271 (1990).
- [12] B. Holdom, Phys. Lett. **B 166**, 196 (1986); R. Foot, H. Lew and R.R. Volkas, Phys. Lett. **B 272**, 67 (1991); I. Antoniadis and K. Benakli, Phys. Lett. **B 295**, 219 (1992); A.Yu. Ignatiev and G.C. Joshi, Phys. Lett. **B 38**, 216 (1996).
- [13] G. Raffelt, Phys. Rep. **320**, 319 (1999).
- [14] M. Marinelli and G. Morpurgo, Phys. Lett. **B 137**, 439 (1984); J. Baumann et al., Phys. Rev. **D 37**, 3107 (1988).
- [15] S.N. Gninenko, N.V. Krasnikov, and A. Rubbia, Phys. Rev. **D 75**, 075014 (2005).
- [16] A. Studenikin, arXiv: 1302.1168 (2013).
- [17] H.B. Li et al., Phys. Rev. Lett. **90**, 131802 (2003); H.T. Wong et al., Phys. Rev. **D 75**, 012001 (2007).
- [18] A.G. Beda et al., Adv. High Energy Phys. **2012**, 350150 (2012).
- [19] M.B. Voloshin, Phys. Rev. Lett. **105**, 201801 (2010), erratum **106**, 059901 (2011); K.A. Kouzakov, A.I. Studenikin, and M.B. Voloshin, Phys. Rev. **D 83**, 113001 (2011).
- [20] J.W. Chen et al., Phys. Rev. **D 88**, 033006 (2013).
- [21] W. Greiner and J. Reinhardt, *Quantum electrodynamics*, Example 3.17, Springer-Verlag (1994).
- [22] B.L. Henke, E.M. Gullikson, and J.C. Davis, At. Data Nucl. Data Tables **54**, 181 (1993).
- [23] H.T. Wong, J. Phys. Conf. Ser. **39**, 266 (2006).
- [24] H.T. Wong, Int. J. Mod. Phys. **D 20**, 1463 (2011); H.B. Li et al., Phys. Rev. Lett. **110**, 261301 (2013); H.B. Li et al., Astropart. Phys. **56**, 1 (2014).